GRUPO LSST AGN - UFRGS

Thaisa Storchi Bergmann

Rogério Riffel

Swayamtrupta Panda

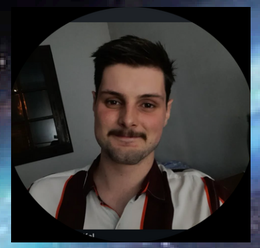

Gabriel Scheffel

Lara Gatto

Gabriel Roier

Vitor Guez

Hygor Benati Gonçalves

Rafaela dos Anjos Oliveira

Marcelo Camaran Lucas

Luiz Matheus Dourado Sanches

UFRGS
UNIVERSIDADE FEDERAL DO RIO GRANDE DO SUL

DEPARTAMENTO DE Astronomia
INSTITUTO DE FÍSICA - UFRGS

NOIRLab/NSF/AURA/J. da Silva

EXPLORING QUASAR VARIABILITY WITH ZTF AT 0<Z<3: A UNIVERSAL RELATION WITH EDDINGTON RATIO

Hygor B. Gonçalves[1], Thaisa Storchi Bergmann[1], Swayamtrupta Panda[2, 3], Edward M. Cackett[4], Michael Eracleous[5]

1) Departamento de Astronomia, Instituto de Física, Universidade Federal do Rio Grande do Sul, CP 15051, 91501-970, Porto Alegre, RS, Brazil
2) International Gemini Observatory/NSF NOIRLab, Casilla 603, La Serena, Chile
3) Laboratório Nacional de Astrofísica (LNA), Rua dos Estados Unidos 154, Bairro das Nações, CEP 37504-364, Itajubá, MG, Brazil
4) Department of Physics and Astronomy, Wayne State University, 666 W. Hancock Street, Detroit, MI 48201, USA
5) Department of Astronomy and Astrophysics and Institute for Gravitation and the Cosmos, Penn State University, 525 Davey Lab, 251 Pollock Road, University Park, PA 16802

Goals

- Study the inner structure (accretion disk and surroundings) of our quasar sample via photometric variability.
- Explore the relationship between photometric variability and fundamental properties of the sample, such as AGN luminosity, Eddington ratio, and black hole mass.
- Use ZTF data as preparatory for the future use of the LSST data.
- Calculate the time delay between photometric bands to derive the physical size of the accretion disk.

Sample

All-**Q**uasar **M**ulti-**E**poch **S**pectroscopy - (**AQMES**):

- The AQMES sample is being monitored within the “Black Hole Mapper” project of the SDSS-V. Among 22 000 quasars of the AQMES sample, we selected to study the photometric variability of the AQMES-MED subsample, that will be observed approximately 10 times over the 4 years of the SDSS-V survey.

- We have selected the quasars that have declinations below 30 deg (so that they could be targets for LSST), resulting in a total **sample of 2058 Type-I quasars** spanning a redshift range from 0 to 3.

Sample

- AQMES WIDE FIELD: ~20,000
- AQMES MEDIUM FIELD: ~2,000
- RM FIELD: ~1,000

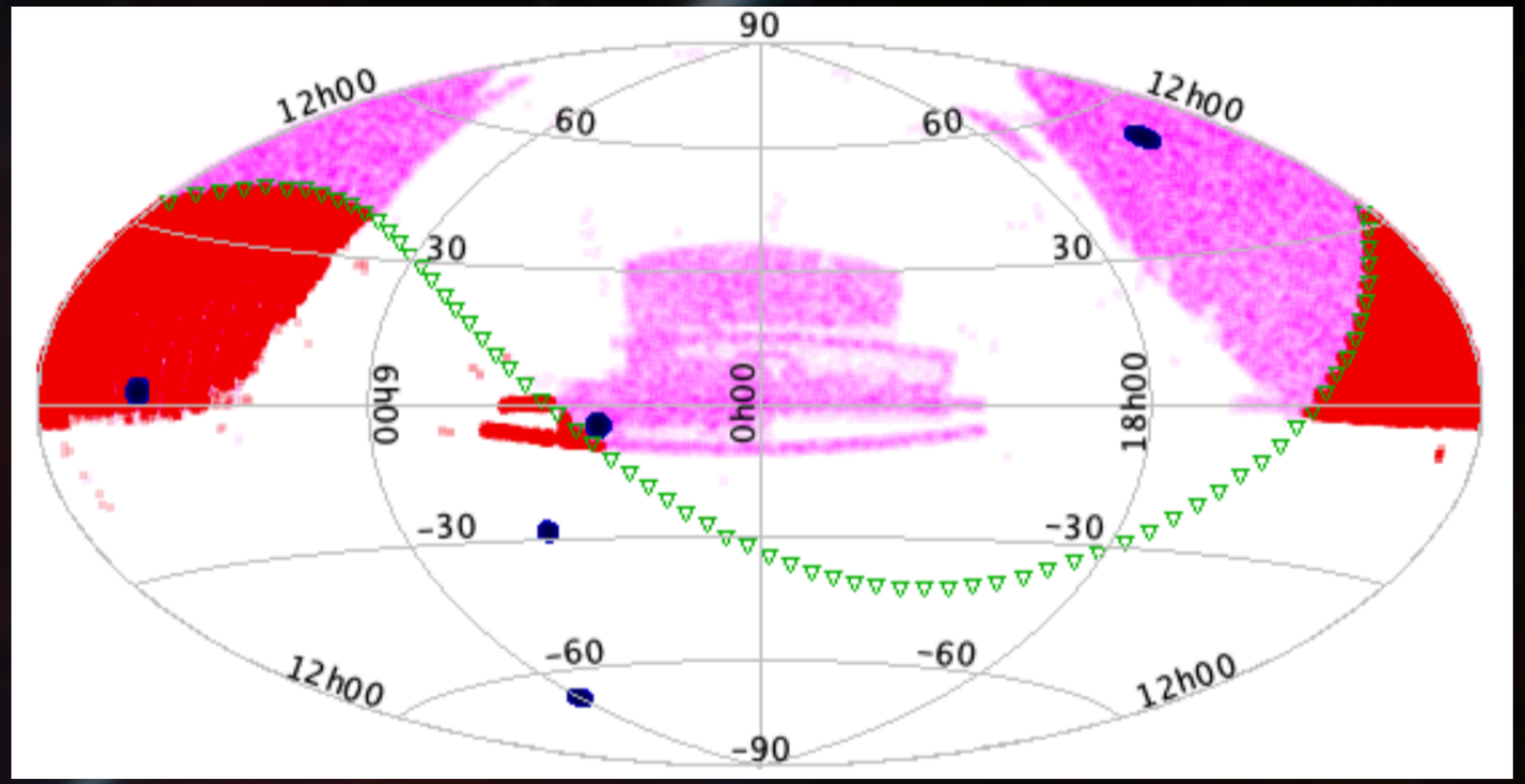

ESO/M. Kornmesser

Zwicky Transient Facility

- ZTF is a fully automated, wide-field survey that systematically explores the optical transient sky. It scans the entire northern sky from the Palomar Observatory every two days.

- Filters and central wavelength:
  - **ztf_g** (4722.74 Å)
  - **ztf_r** (6339.61 Å)
  - **ztf_i** (7829.03 Å)

Palomar Observatory/Caltech

ZTF filters at a glance

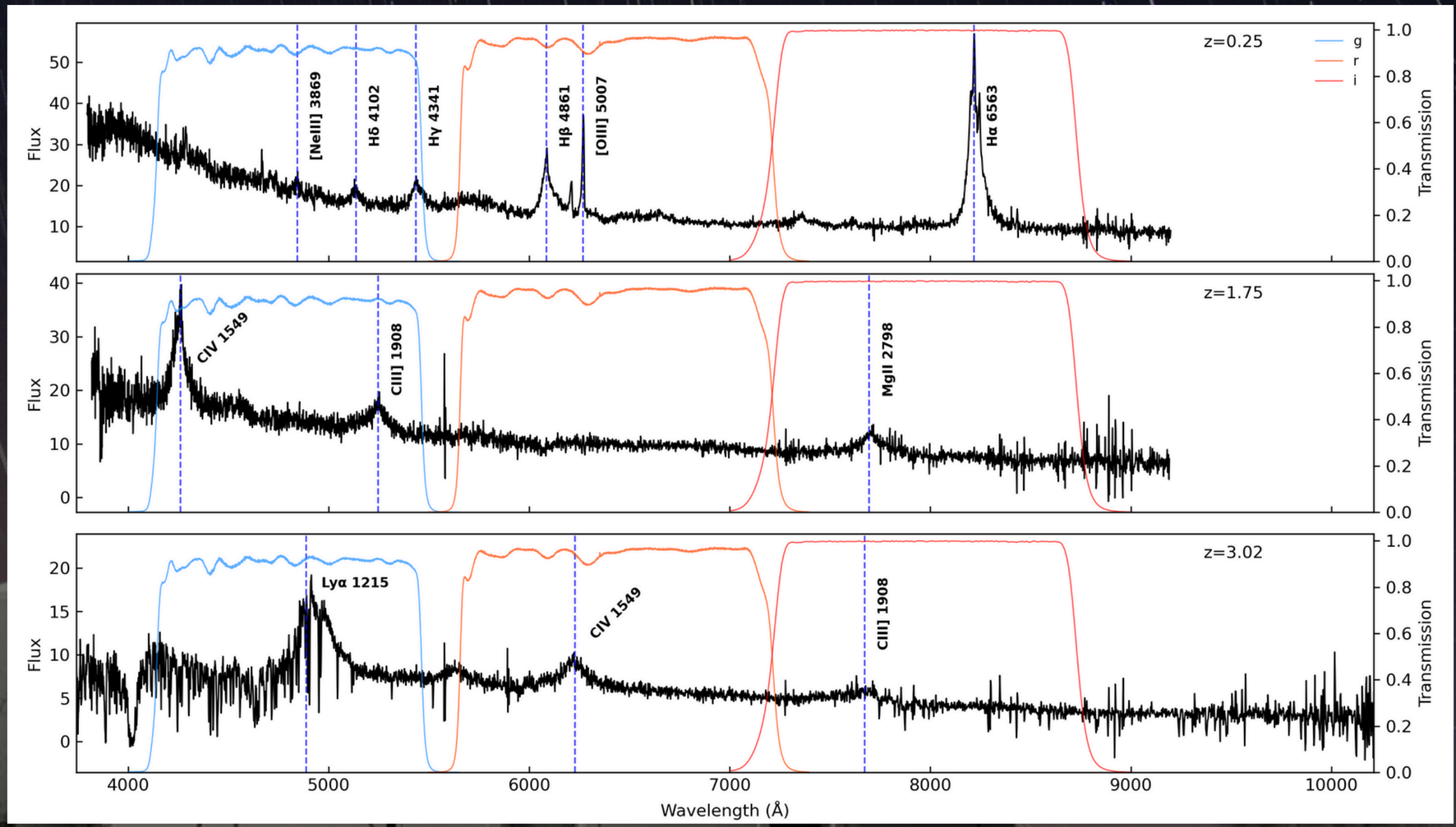

Benati Gonçalves et al. (in prep.)

Data filtering

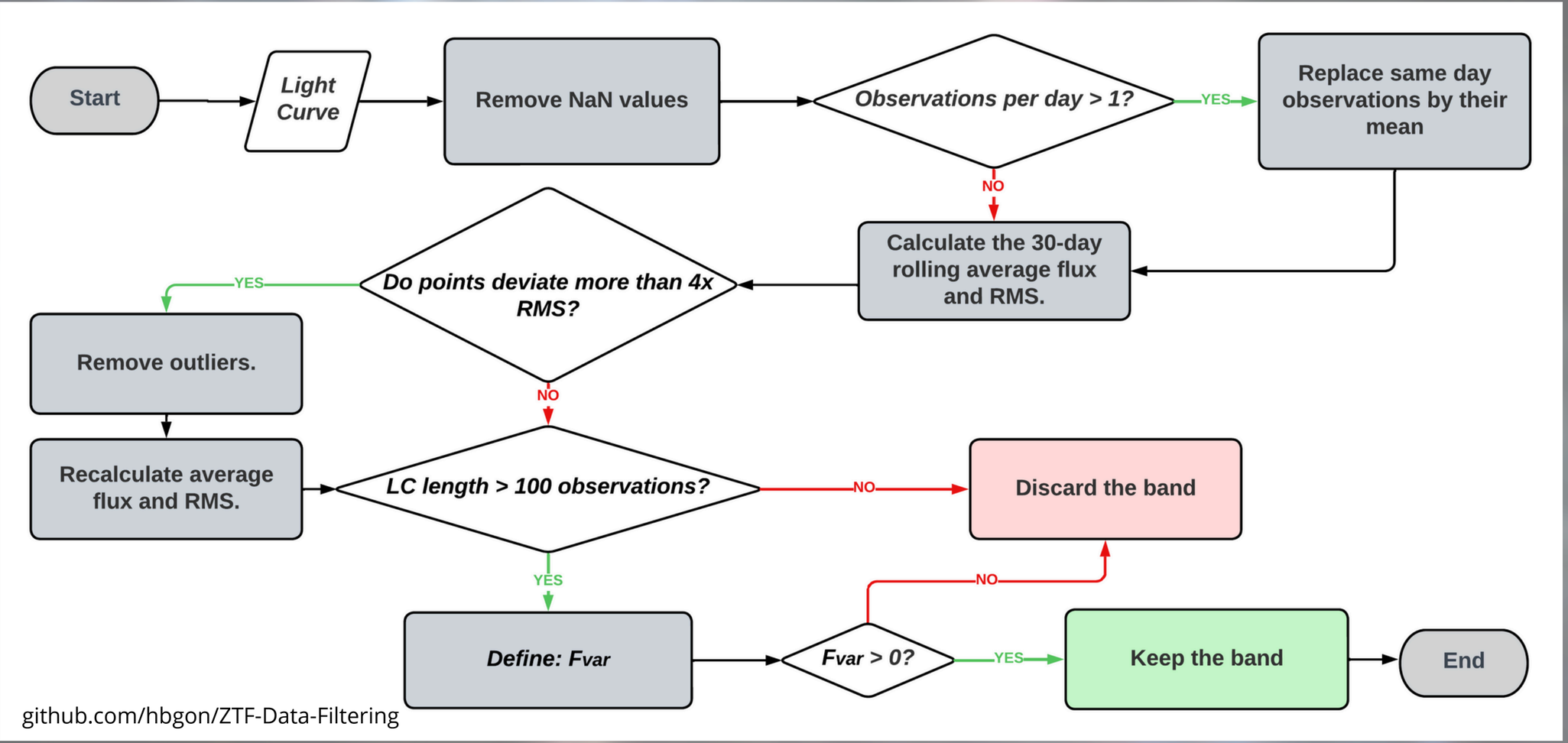

Benati Gonçalves et al. (in prep.)

NASA, ESA and J. Olmsted (STScI)

Data filtering

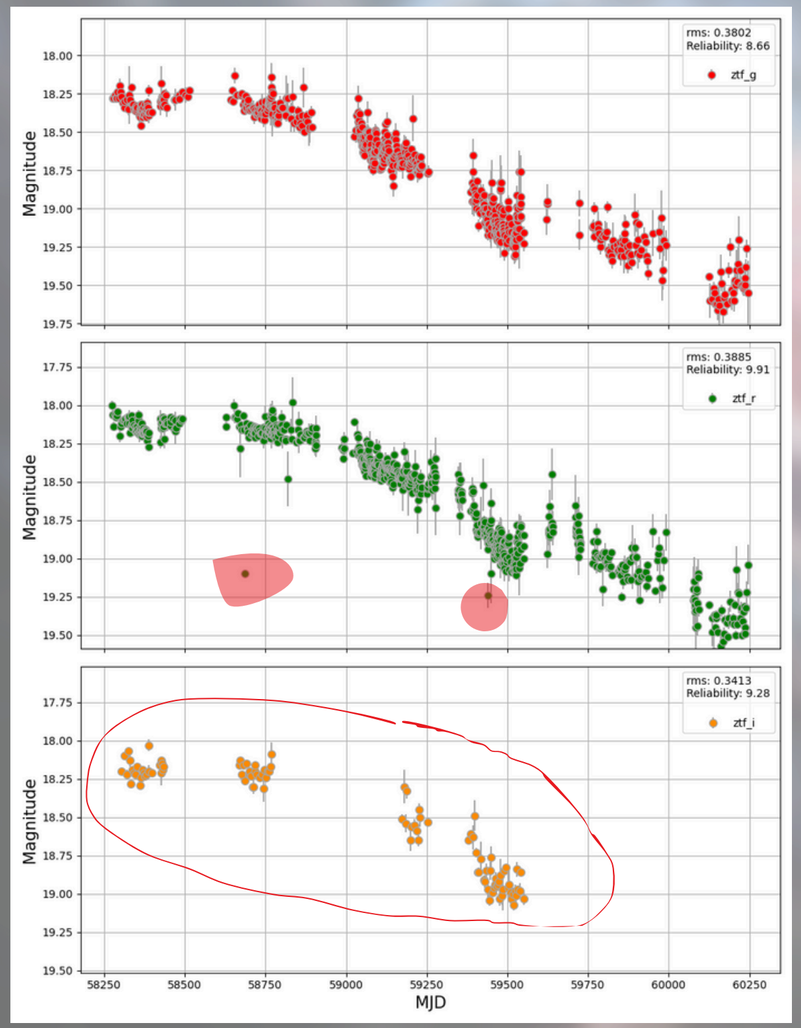

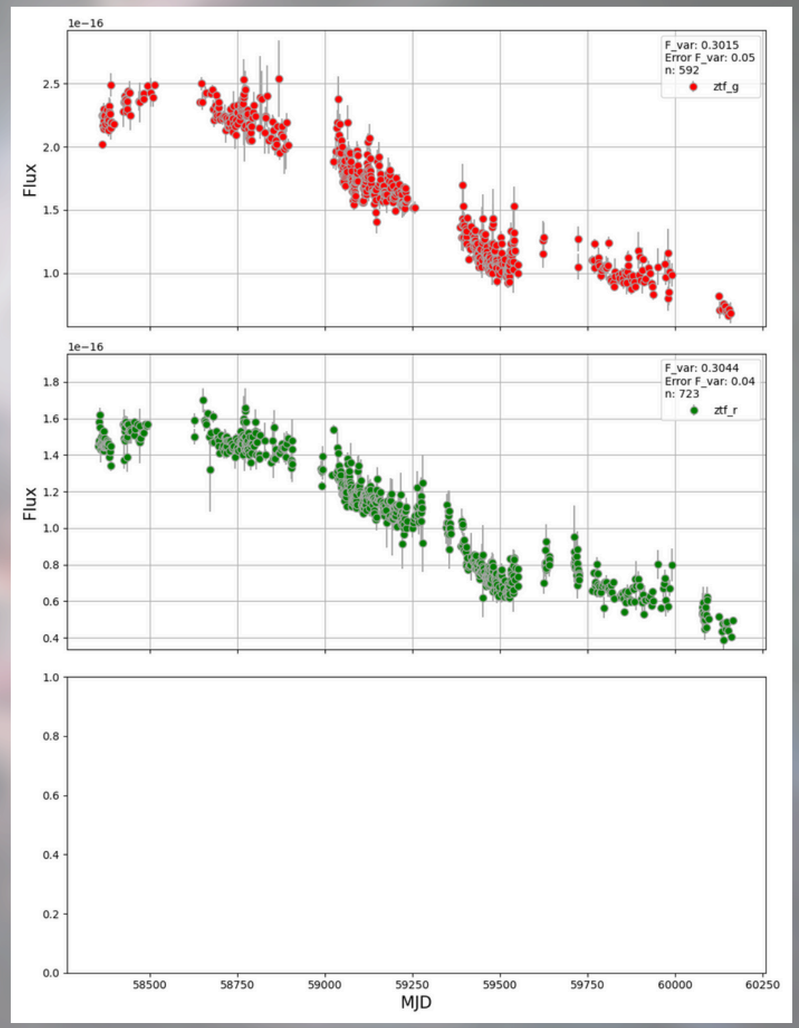

NASA, ESA and J. Olmsted (STScI)

Data filtering

A common parameter to characterize variability is the mean fractional variation,

$$F_{\rm var} = \frac{\sqrt{\sigma^2 - \delta^2}}{\langle f \rangle} \quad ,$$

where the quantities are (a) the mean flux for all N observations,

$$\langle f \rangle = \sum_{i=1}^{N} f_i \quad ,$$

(b) the variance of the flux (as observed),

$$\sigma^2 = \frac{1}{N} \sum_{i=1}^{N} (f_i - \langle f \rangle)^2 \quad ,$$

and (c) the mean square uncertainty of the fluxes

$$\delta^2 = \frac{1}{N} \sum_{i=1}^{N} \delta_i^2 \quad .$$

Peterson, B. M. (2001). Variability of active galactic nuclei. In Advanced Lectures on the Starburst-AGN Connection (pp. 3-68).

Results

Total sample after filtering process:

- g-band **919**
- r-band **911**

In order to analyze how properties vary across cosmic time, we divided our data into four redshift bins. We chose the g-band as our reference due to its significant variability and extensive coverage.

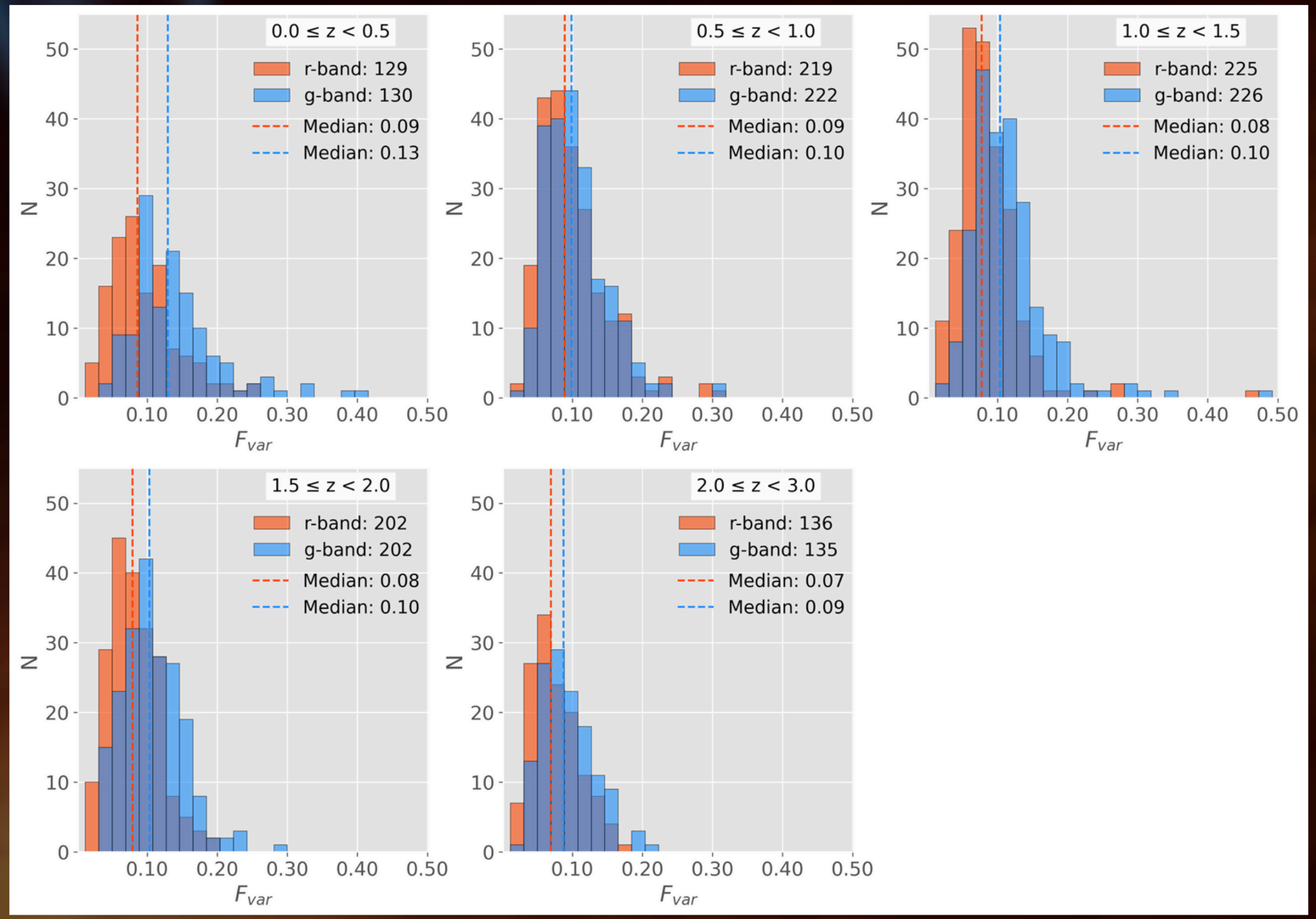

Benati Gonçalves et al. (in prep.)

Results

- For our filtered sample of 915 quasars, we performed a cross-match with the SDSS DR16 quasar catalog (Wu & Shen, 2022) to characterize the sample. Some properties are highlighted bellow:

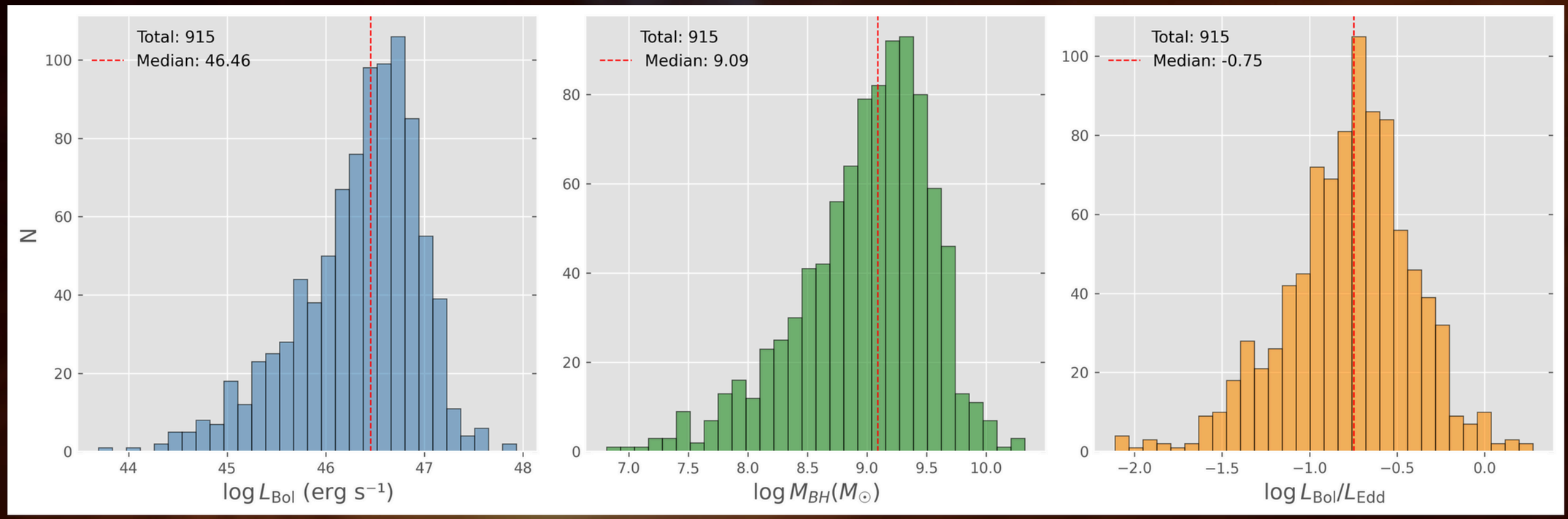

Benati Gonçalves et al. (in prep.)

Results

Absolute magnitude in the g-band (M_g) and redshift (z) distributions for our sample:

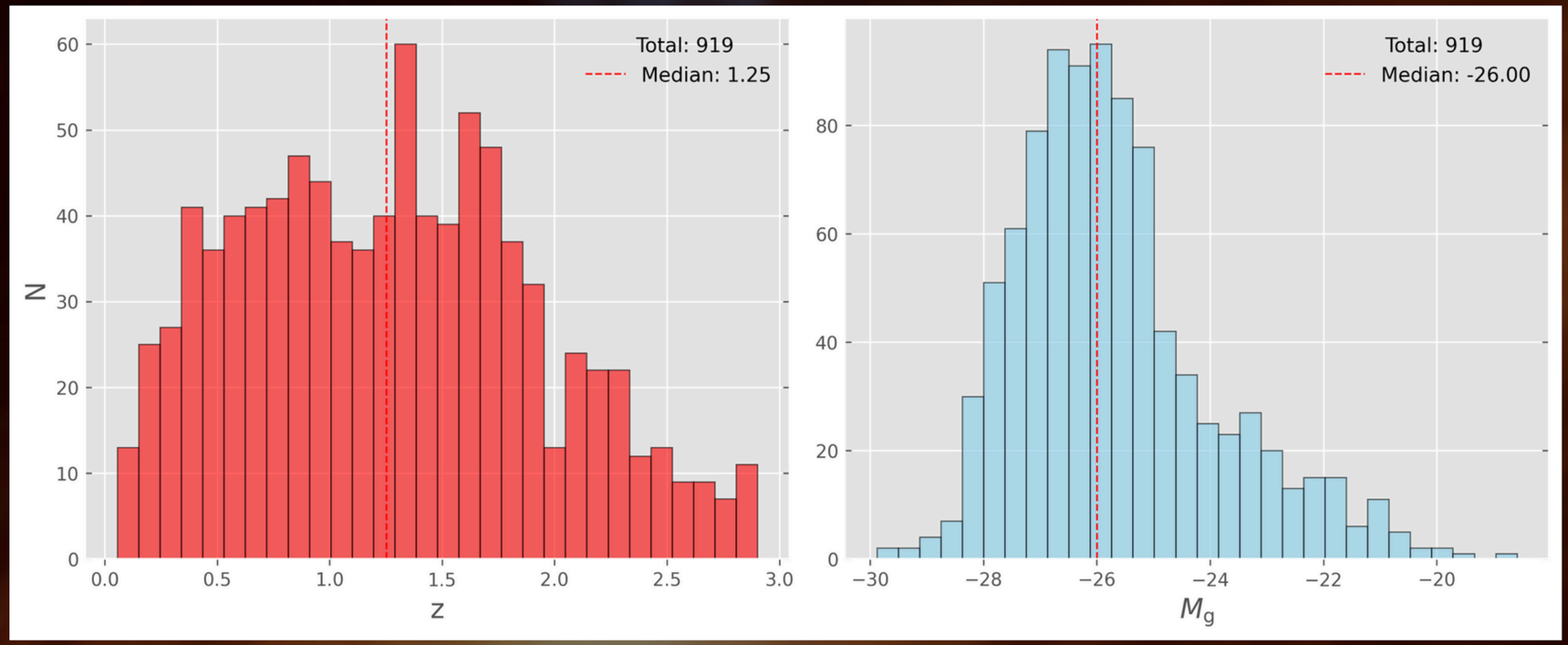

Benati Gonçalves et al. (in prep.)

Results

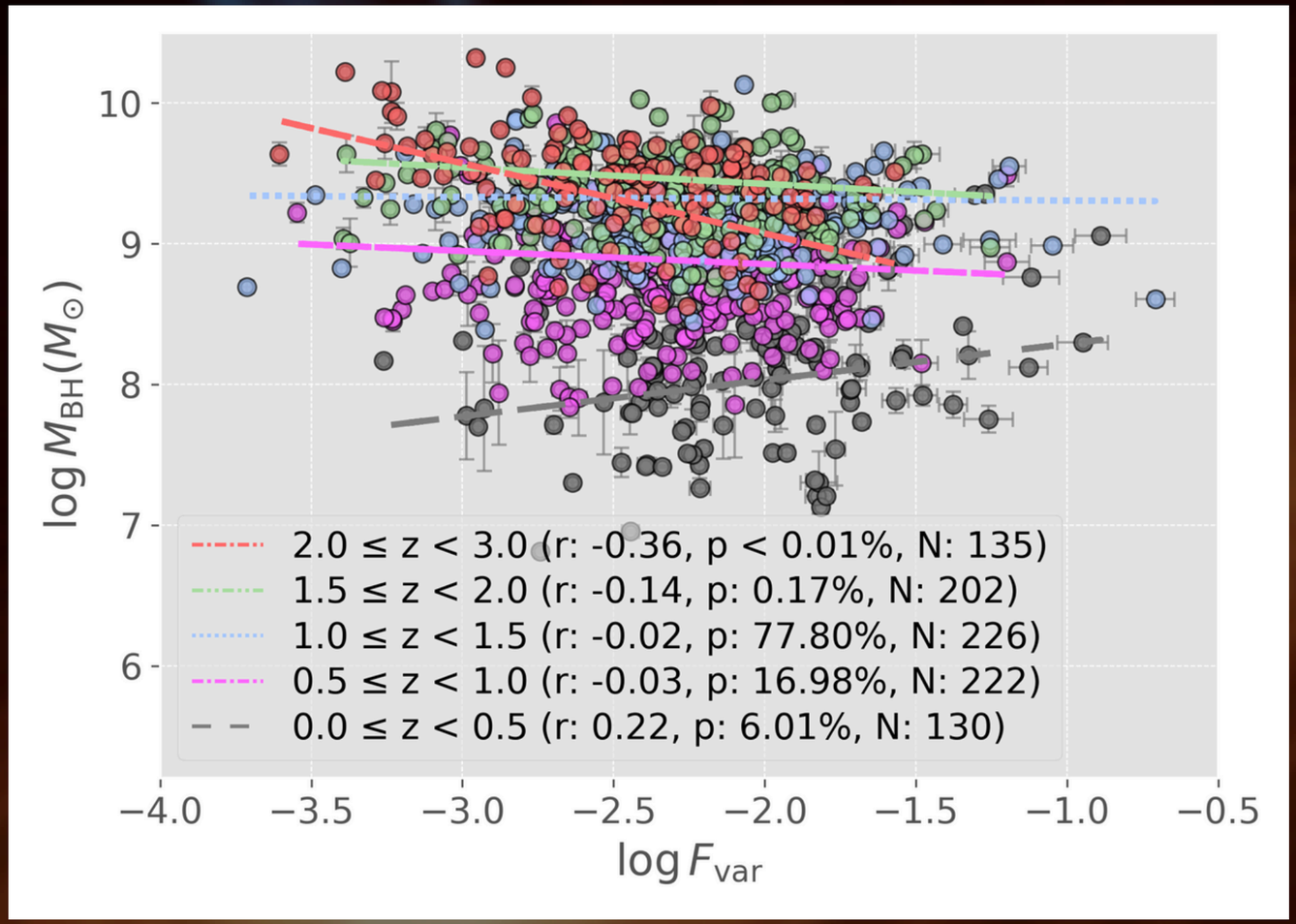

Benati Gonçalves et al. (in prep.)

Results

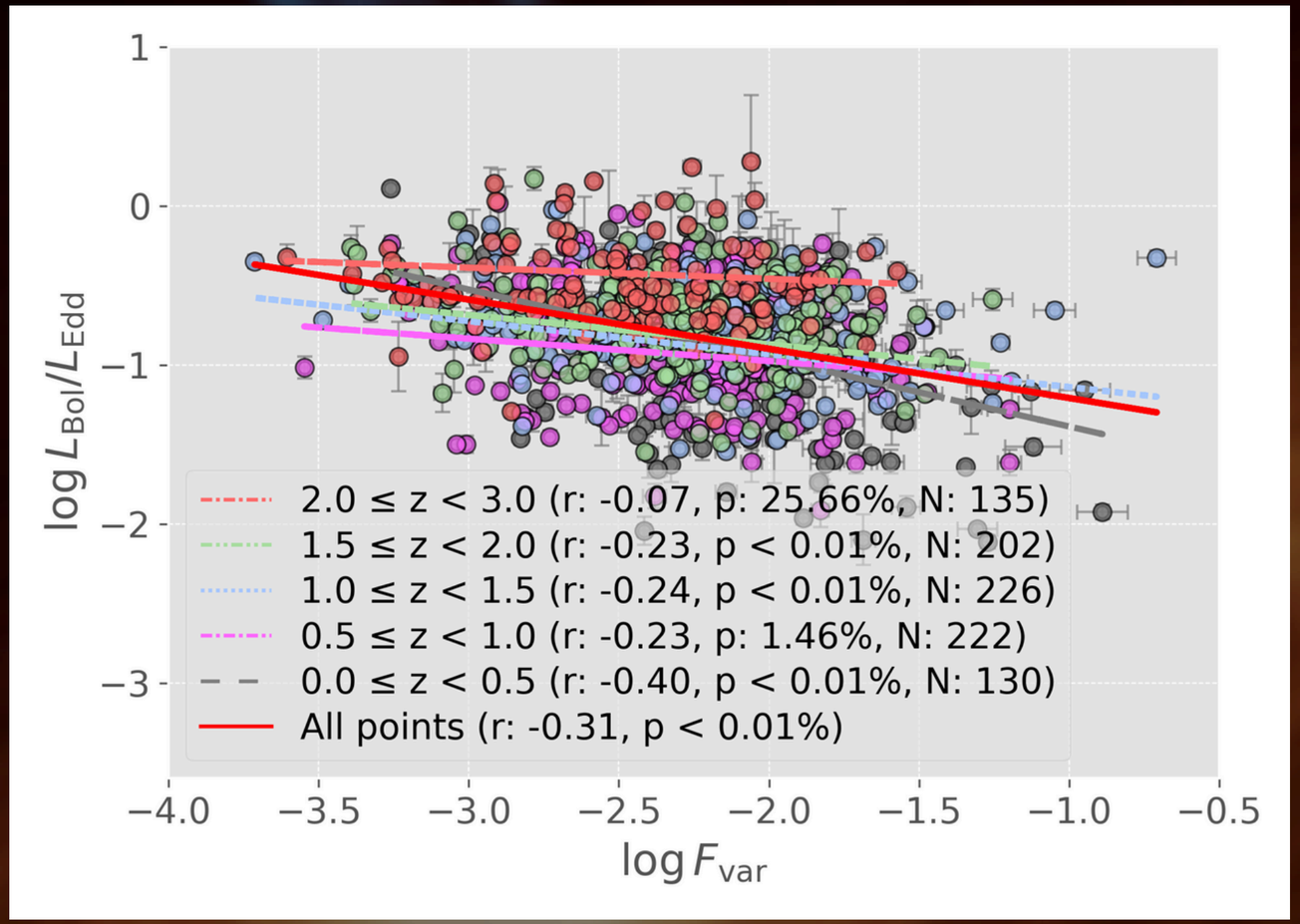

Benati Gonçalves et al. (in prep.)

Results

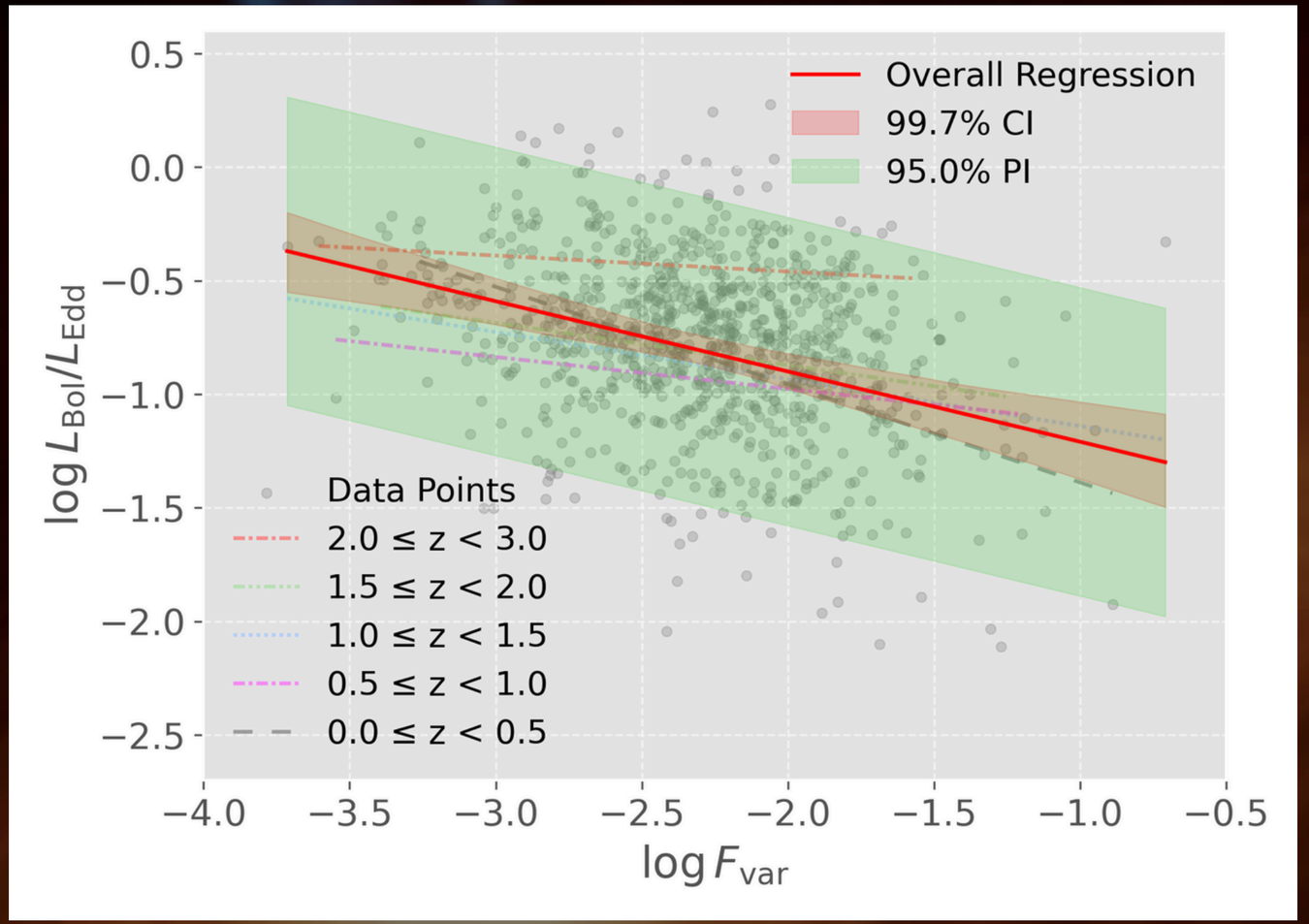

Benati Gonçalves et al. (in prep.)

Conclusions

- We observed a consistent anti-correlation between the variability (F_var) and continuum luminosities (e.g., L_1350, L_3000, L_5100), extending also to bolometric luminosity. This reaffirms the universality of the relationship. Additionally, as expected, there is no correlation between F_var and [OIII] emission, which aligns with the understanding that the narrow line region does not vary within the 6-year observation period.

- The relationship between F_var and black hole mass shifts from a weak positive correlation at low redshifts to a robust anti-correlation at higher redshifts.

- A persistent anti-correlation exists between the Eddington ratio and F_var across all redshifts, with a trend of r = -0.31 and the strongest correlation at the lowest redshift (r = -0.40). Using the complete sample, a linear relationship was obtained with high significance.

NASA/Artsiom P

Thank you!

github.com/hbgon

hygor.benati@ufgrs.br

Appendix

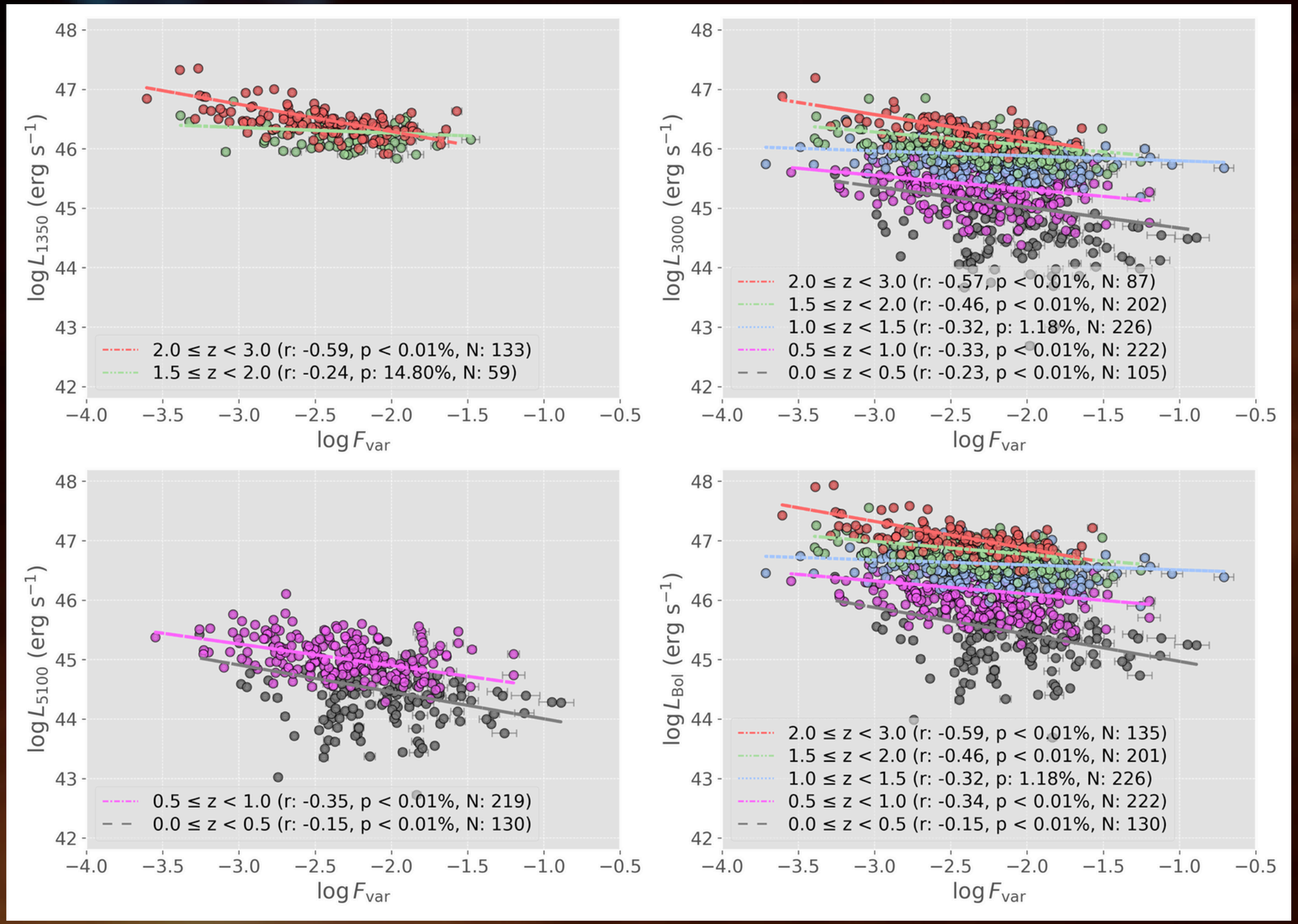

Benati Gonçalves et al. (in prep.)

1. Ten highly variable and reliable sources were chosen.
2. PyROA (Donnan et al. 2021) was used on each source, resulting in initial time delay estimates.
3. Further refinement of the program will be conducted, incorporating additional methods such as JAVELIN and PyCCF.
4. The initial time delays vary from hours to light-weeks between the g and r bands.

RA (°)	DEC (°)	g_band cadence	Rel. g	rms_g	delay_gr	delay_gi
1.127167	25.730611	546	4.933698	0.252724	$3.23^{+0.99}_{-1.06}$	None
0.501000	26.030111	584	5.683474	0.229971	$-0.8^{+1.43}_{-1.54}$	$2.43^{+4.04}_{-3.91}$
10.127792	25.335083	655	8.664237	0.380179	$0.20^{+1.30}_{-1.36}$	$-6.93^{+3.19}_{-3.00}$
10.832250	0.854278	534	12.040972	0.355799	$2.29^{+0.92}_{-0.88}$	None
5.929083	1.045250	508	4.892831	0.189204	$-2.75^{+1.72}_{-1.71}$	None
343.280667	19.709611	1028	8.471564	0.186710	$7.07^{+0.48}_{-0.50}$	$9.57^{+1.09}_{-1.06}$
335.625667	1.042056	523	4.231039	0.255656	$0.13^{+0.91}_{-0.92}$	None
10.101625	25.717611	647	4.479121	0.241477	$-3.96^{+1.56}_{-1.66}$	None
8.806042	24.538417	601	4.413962	0.244720	$0.82^{+0.66}_{-0.65}$	None
33.445750	-2.941944	693	8.286984	0.205730	$1.90^{+0.63}_{-0.68}$	None